Reduction of Background Activity Through Radiolabeling of Antifibrin Fab' with ^{99m}Tc-Dextran

Bruce R. Line, Peter B. Weber, Roberta Lukasiewicz, and Raymond N. Dansereau

Departments of Radiology, Pharmacy, and Biochemistry, Albany Medical Center, Albany, New York

Scintigraphic detection of occult disease is limited by background activity in the blood and in the extravascular space that reduces target-specific contrast. To lower nonspecific background activity, we have studied the in vivo biodistribution kinetics of a clot-targeting molecule (MH1 Fab') attached to ^{99m}Tc-dextran. We tested the hypothesis that the complex will have better background clearance than the directly radiolabeled clot-targeting molecule. **Methods:** Fab' fragments of MH1 Fab' antifibrin antibody were coupled to ^{99m}Tc-sulfhydryl dextran through disulfide exchange, and clot binding bioreactivity was tested in vitro and in vivo in a rabbit jugular vein thrombus model. To assess the background clearance kinetics and extravascular leakage, we studied ^{99m}Tc-dextran, ^{99m}Tc-MH1 Fab', and the ^{99m}Tc-dextran–labeled MH1 Fab' complexes in rats. **Results:** ^{99m}Tc-radiolabeled dextran derivatives were radiochemically stable and retained clot-binding bioreactivity in vivo. In the rat model, blood and tissue clearance of the ^{99m}Tc-dextran MH1 Fab' constructs was substantially improved relative to directly radiolabeled MH1 Fab'. At 1 h, total and extravascular tracer localizations in lung and muscle were significantly lower for ^{99m}Tc-dextran–radiolabeled MH1 Fab' than for ^{99m}Tc-MH1 Fab' ($P < 0.05$). **Conclusion:** The study observations suggest that radiolabeling through a ^{99m}Tc-dextran moiety may improve the detection of pulmonary emboli and other clinically important fixed intravascular targets by lowering nonspecific background activity.

Key Words: image background; dextran; radiopharmaceutical; antifibrin antibody; intravascular targeting

J Nucl Med 2000; 41:1264–1270

Thromboembolic disease, inflammation, neoplasia, and atherosclerotic disease all manifest unique molecular features on the endothelium or at fixed intravascular sites. Because of their location, these targets do not require extravascular tracer migration to be detected scintigraphically. Target detection may be further enhanced if nontargeted tracer can be held captive to, and yet rapidly cleared from, the intravascular space.

Because of the molecular properties of ^{99m}Tc-dextran, we have studied it as a way to achieve a high target-to-background ratio. The dextran molecule is hydrophilic, so it does not easily leak through the lipid endothelial barrier (*1–3*). The molecule is also metabolized by the liver and excreted through the kidneys (*3,4*); therefore, ^{99m}Tc-dextran will likely be retained within, yet cleared from, the intravascular pool. In addition, the hepatic site of dextran metabolism (*3–6*) provides a way to selectively break down nontargeted radiopharmaceuticals.

We hypothesized that relative to their directly labeled counterparts, intravascular targeting molecules indirectly radiolabeled with ^{99m}Tc-dextran should have lower background activity and, hence, a higher target-to-background ratio. To test the hypothesis, we developed biochemical methods to manipulate the dextran chain and introduce some modifications through which a targeting molecule could be attached. We coupled MH1 Fab' antifibrin to the dextran derivative, evaluated the bioreactivity of the attached antibody, and radiolabeled the dextran portion of the complex. Finally, we studied the in vivo biodistribution and clearance of ^{99m}Tc-dextran-MH1 Fab' relative to ^{99m}Tc-MH1 Fab' to verify the usefulness of dextran radiolabeling in reducing image background activity.

MATERIALS AND METHODS

MH1 Antifibrin Antibody Radiolabeling

^{99m}Tc-labeled Fab' monoclonal antibody (^{99m}Tc-MH1) recognizes cross-linked fibrin and does not recognize fibrinogen or fibrin degradation products. The investigational product MH1 Fab' (product lot RPL01-92324; American Biogenetic Sciences, Inc., Copiague, NY) was supplied in sterile evacuated reaction vials containing 0.5 mg lyophilized nonpyrogenic antifibrin MH1 Fab' antibody fragment with stannous chloride in a phosphate buffer. Radiolabeling was performed according to manufacturer instructions by aseptically adding 740 MBq sodium pertechnetate to the reaction vial. The final volume of 2.0 mL was obtained by adding 0.9% sodium chloride. The contents were mixed for 15 s and allowed to stand for 3 min. The radiochemical purity of ^{99m}Tc-labeled MH1 Fab' was determined by instant thin-layer chromatography using an SG strip (Pall Gelman Laboratory, Ann Arbor, MI) in a solution of 10% trichloroacetic acid. The labeling efficiency was always greater than 90%.

Received Mar. 1, 1999; revision accepted Oct. 27, 1999.

For correspondence or reprints contact: Bruce R. Line, MD, Nuclear Medicine, A-72, Albany Medical Center, Albany, NY 12208.

Construction and Radiolabeling of Dextran Complexes

A 6% solution of dextran in 0.9% sodium chloride (Gentran 70; Baxter Healthcare, Irvine, CA) was composed of stock dextran (Kabi Pharmacia Diagnostics, Piscataway, NJ) having an average molecular weight of 69,300. Five hundred milliliters Gentran 70 were freed of salts by 3 cycles of precipitation in an equal volume of 95% ethanol followed by resuspension in triple-distilled, deionized water. The third precipitate was resuspended in 100 mL water. A homogeneous final precipitate was formed in a blender by slowly adding the dextran suspension to 600 mL 95% ethanol. The precipitate was collected on a glass sinter funnel under argon. The cake was then rehomogenized with 250 mL t-butanol and freeze dried.

The dextran isolate was aminated through azide reduction to introduce a limited number of amino groups to the backbone. This modification provided sites for coupling targeting molecules and tracer ligands to dextran without weakening the integrity of the dextran backbone or significantly modifying the chain. The dextran was first tresylated in pyridine, with the tresyl groups replaced with sodium azide in hot methylsulfoxide. After sodium azide replacement of the tresyl groups, the azido moieties were reduced with 1,3-dimercaptopropane (*7*). The desired tresylation level was achieved by adding a 10% excess of tresyl chloride to a mixture of dextran in anhydrous dimethylsulfoxide and anhydrous triethylamine. To this end, the dry dextran was dissolved to a 5% concentration in dimethylsulfoxide and cooled to −15° to −20°C. Triethylamine was added slowly over 30 min to achieve a 15% excess over the tresyl chloride. After an additional 15 min of reaction, the mixture was precipitated with 10 volumes of acetone. The gel was washed twice in 10 volumes of dry acetone, once in acidified acetone (10% 1 mol/L HCl) and again in dry acetone. Gram quantities of aminodextran derivative were produced in an 80%–90% yield. The degree of substitution of the aminodextran derivatives was determined through measurement of intact hexose content with the phenol-sulfuric acid method (*8*), and the amino group content was analyzed using trinitrobenzene sulfonic acid (*9*). The method introduced 5–20 amino groups per 70-kDa dextran molecule.

Preparation of ^{99m}Tc-Thiol Dextran. To produce thiolated dextran (Fig. 1), 0.5–1 g aminodextran was suspended in a saturated bicarbonate buffer concentration of 100 mg per milliliter. A 50:1 molar excess of *S*-acetyl mercaptosuccinic anhydride dissolved in acetone was added dropwise to the rapidly stirred aminodextran solution, using 0.2 mol/L NaOH to maintain the pH between 6.5 and 8. After 20 min, 5 mL 1 mol/L sodium acetate were added, and the pH was reduced to 5.5 with 0.2 mol/L HCl. The product was precipitated in 95% ethanol, redissolved in 10 mL distilled water, gel filtered over a PD10 column with Sephadex G-25 (Kabil Diagnostics Pharmacia), and lyophilized. To radiolabel the thiolated dextran, the *S*-acetyl mercapto group was deprotected over 2–4 min at pH 11–12 followed by neutralization. This product was combined with 100 μg stannous chloride dihydrate ($SnCl_2 \cdot 2H_2O$; Sigma Chemical Company, St. Louis, MO) and 200 μg ethylenediaminetetraacetic acid (Sigma), and 100–200 MBq ^{99m}Tc were added. The radiolabeled dextran was isolated by gel filtration over a Sephadex G-25 column. To show thiol-specific coupling of ^{99m}Tc, aliquots of ^{99m}Tc-dextran 70 and ^{99m}Tc-thiol dextran were maintained under N_2 in the presence of a 1750× molar excess of glucose, diethylenetriaminepentaacetic acid (DTPA), or L-cysteine (*10*). Binding to the polysaccharide compounds after 2 and 4 h of exposure was determined by adding a 0.2-mL aliquot of sample to a G-25 column that was pre-equilibrated and eluted with 0.9% NaCl (aqueous) (*11*).

Preparation of ^{99m}Tc-Dextran-HSA and ^{99m}Tc-Dextran-MH1 Fab'. Human serum albumin (HSA) was combined with a 2-fold molar excess of 2-iminothiolane (Sigma) in the presence of a 10-fold molar excess of 2,2' dithiodipyridine (Sigma) at pH 7.0 for 2 h at room temperature. The product was gel filtered through a G-25 column in 50 mmol/L Tris buffer and incubated for 15 min with a 1:1 molar quantity of ^{99m}Tc-thiol dextran. Greater than 80% coupling of the dextran and HSA was typically achieved, gauged by the release of pyridine-2-thione measured spectrographically at 343 nm.

^{99m}Tc-dextran-MH1 Fab' was prepared by combining freshly reduced MH1 Fab' with dithiodipyridine-activated ^{99m}Tc-thiol dextran. The MH1 $F(ab')_2$ was reduced to the Fab' fragment of the antibody by incubation with a 1000 molar excess of β-mercaptoethanol for 45 min at room temperature. The Fab' fragment was purified by Sephadex G-10 gel chromatography in an oxygen-free environment. The mobile phase was 0.9% sodium chloride, pH 7.0.

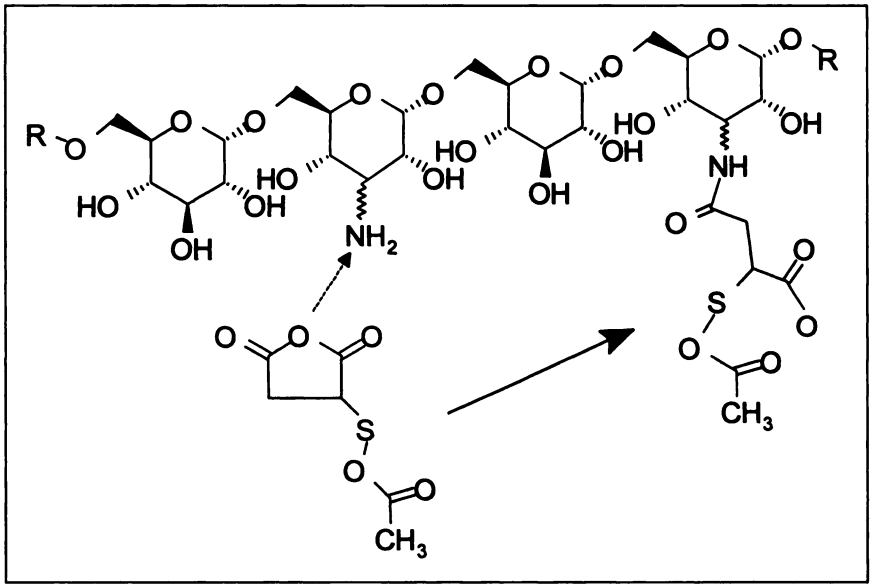

FIGURE 1. Synthesis of thiol dextran shows interaction of *S*-acetyl mercaptosuccinic anhydride with aminodextran to produce acetyl-protected thiol-derivatized dextran chain. Protecting group was removed before ^{99m}Tc radiolabeling of dextran complex.

^{99m}Tc-thiol dextran was combined with a 2:1 molar excess of 2,2′ dithiodipyridine and gel filtered through a G-25 column in 50 mmol/L Tris buffer. Both products were combined in a 1:1 molar ratio, and the coupling was followed by the release of pyridine-2-thione.

Verification of ^{99m}Tc-Dextran-MH1 Fab′ In Vitro and In Vivo Clot Binding

The functional integrity of ^{99m}Tc-dextran-MH1 Fab′ was evaluated in a clot-binding assay (*12*). The test agent (10–20 μg) was added to a mixture of 0.5 mL Tris buffer, 0.5 mL acid citrate dextrose–preserved plasma, and 12 μL 1 mol/L $CaCl_2$ in a microcentrifuge tube. Clots were formed by rapidly mixing the solution with 6 units of thrombin. After 10 min of room temperature incubation, the clot mass was separated from unbound activity by centrifugation and washing of the compressed clot mass. The assay measures the fraction of the radiolabeled dextran molecules that were coupled to bioreactive and functionally oriented MH1 Fab′ molecules. Clot binding was expressed as a percentage of the added radioactivity. Controls included ^{99m}Tc-thiolated dextran not linked to MH1 Fab′ and ^{99m}Tc-MH1 Fab′ not bound to dextran.

In vivo studies in New Zealand white rabbits were performed to confirm the in vivo functional integrity of ^{99m}Tc-dextran-MH1 Fab′. New Zealand white rabbits (Marland Breeding Farms, Inc., Hewitt, NJ) weighing approximately 3 kg were anesthetized, and an external jugular vein was exposed from the anterior bifurcation to the junction of the transverse and external jugular veins. The vein was temporarily occluded with a ligature near its lower exposed margin. A 2-cm segment of wool knitting yarn soaked in thrombin solution (100 NIH units/mL) was introduced into the lumen of the ligated segment with a sterile needle. The clot was allowed to age for a minimum of 45 min, and the ligature on the jugular vein was released. The animals were then positioned supine on a gamma camera with a rectangular field of view, the test tracer was injected, and serial 5-min images were obtained for 2 h. Image regions of interest were placed over the cervical clot, contralateral neck region, lung, heart, and liver to assess clot-to-background and clot-to-organ ratios.

Biodistribution and Compartmental Testing of ^{99m}Tc-Radiolabeled Compounds in a Rat Model

To assess background clearance kinetics and extravascular leakage, ^{99m}Tc-dextran 70, ^{99m}Tc-gluceptate (Mallinckrodt, Inc., St. Louis, MO), and the pilot dextran-labeled complexes were studied in a rat model developed in our laboratory (*13*). Sprague-Dawley rats (250- to 300-g body weight) received an injection of 30–50 MBq ^{99m}Tc-radiolabeled test agent, and sequential 5-min mode images (128 × 128 bytes) were obtained. After imaging, each rat was injected with 0.5 mL (20–40 kBq) ^{125}I-HSA (Mallinckrodt) to determine the partitioning of ^{99m}Tc-labeled tracer molecules between tissue and blood compartments in necropsy tissue samples (*13*). Three minutes later, a 0.5-mL intracardiac blood sample was obtained, and the rat was killed.

Regions of interest (5 × 5 pixels) over the heart, lung, liver, kidneys, thigh, and bladder were used to plot organ activity kinetics over the first hour of imaging. The activity within the region of interest for each of the 12 5-min imaging intervals was decay corrected and expressed as a percentage of total animal activity. The 0- to 60-min integral of tracer activity was used as an index to compare the tracer compounds. To reduce errors associated with differences in injection time, the raw curves were fit to a 2-compartment model and the area under the 1-h clearance curve was derived from the sums of the integrals of the compartments.

Necropsy tissue samples ranging from 0.5 to 1.0 g obtained from the blood, lung, heart, liver, spleen, kidney, and muscle were assayed in a γ well counter with multichannel analyzer windows centered over the peaks for ^{99m}Tc and ^{125}I. Isotope counts were adjusted for sample weight, channel scatter crossover, and radionuclide decay. Calculations were normalized for administered activity, as determined from activity standards and injected volume. The activity ratio of the ^{125}I-HSA and ^{99m}Tc tracers in a blood sample was used to compute the quantity of ^{99m}Tc tracer outside the vascular and capillary blood in necropsy tissue samples (*13*). The specific distribution of tracer to the intravascular versus extravascular (non–blood-pool) compartments was determined using the tissue blood fraction as defined from the ratio of ^{125}I counts in a gram of tissue to that in a gram of blood. The ^{99m}Tc activity in blood was then used to determine the intravascular ^{99m}Tc in each tissue sample. The extravascular ^{99m}Tc activity was found by subtracting the intravascular ^{99m}Tc activity from the total ^{99m}Tc in the tissue sample (*13*).

ANOVA was performed with multiple comparisons using the Newman-Keuls test. Significance was accepted at the $\alpha = 0.05$ level.

RESULTS

The ^{99m}Tc-dextran-MH1 Fab′ had 96.4% ± 2.7% labeling efficiency and binding stabilities of 95.7% ± 3.0% and 96.1% ± 3.1% 6 h after labeling. Clear enhancement of the ^{99m}Tc-binding stability of thiol dextran relative to dextran was attributable to the presence of the mercaptosuccinic side group (Fig. 1). The glucose challenge results suggest that ^{99m}Tc binding at the thiol function was stronger than that of the remainder of the dextran chain and that the dextran mercaptosuccinate complex had a higher affinity for technetium than did DTPA (Fig. 2). As expected, the thiol group is overwhelmed by the large excess (1750 times) of L-cysteine.

The in vitro clot-binding assay measured the fraction of the radiolabeled dextran molecules that was coupled to bioreactive and functionally oriented MH1 Fab′ molecules. Clot binding expressed as a percentage of the added radioactivity was 0.77% ± 0.38% for ^{99m}Tc-thiol dextran, 0.89% ± 0.43% for ^{99m}Tc-dextran-HSA, 90.6% ± 1.30% for ^{99m}Tc-MH1 Fab′, and 84.3% ± 2.5% for ^{99m}Tc-dextran-MH1 Fab′. The in vivo clot-binding studies performed with ^{99m}Tc-dextran-MH1 Fab′ in rabbits showed good soft-tissue background clearance by 30 min and nearly complete blood-pool clearance by 2 h as reflected by reduced cardiac activity (Fig. 3). The thrombus in the left cervical region was clearly evident by 30 min. The ratio of the thrombus to the contralateral neck region was 9.9, and the ratio of the clot to the heart blood pool was 1.3.

In the rat biodistribution and necropsy studies, the total and extravascular percentage injected dose per gram of tissue (%ID/g) were compared for the lung, heart, muscle, and liver (Table 1). In the heart blood pool and liver parenchyma, image activities for the ^{99m}Tc-dextran–labeled complexes were significantly lower than for ^{99m}Tc-MH1

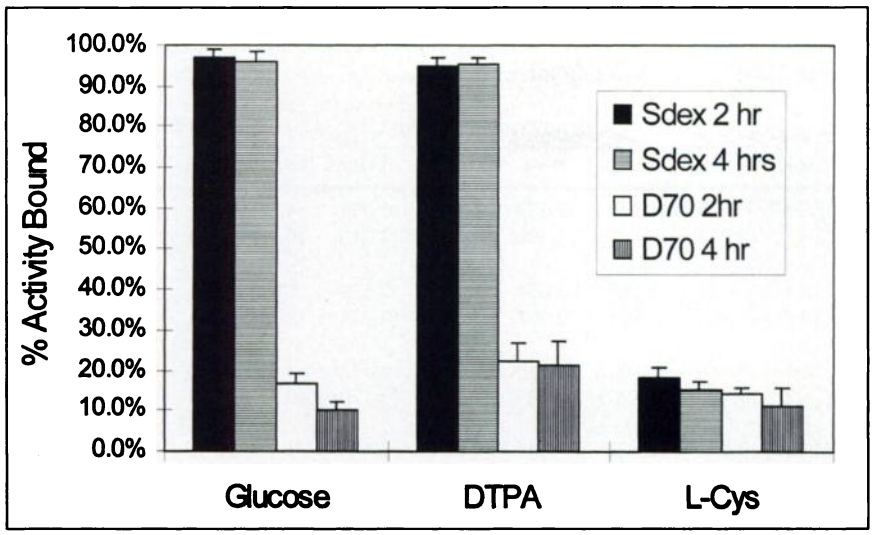

FIGURE 2. ^{99m}Tc label stability studies show percentage binding after 2- and 4-h incubation of thiol dextran and native dextran with 1750× molar excess of glucose, DTPA, and L-cysteine (L-Cys) competition. Values are mean ± SD of 3 measurements. D70 = dextrose 70; Sdex = thiol dextran.

Fab′. The image-derived indices showed a significant improvement of background clearance related to ^{99m}Tc-dextran labeling. The total necropsy activity in the lung was lowest for ^{99m}Tc-GHA, a small molecule that is rapidly excreted by the kidneys. ^{99m}Tc-thiol dextran and the proteins radiolabeled through dextran derivatives showed low total and extravascular activity for the lung, heart, and muscle. These values were substantially lower than the comparable values for ^{99m}Tc-MH1 Fab′. The areas under the curve for ^{99m}Tc-GHA and the other pilot compounds are shown in Table 1. The lung image activities for ^{99m}Tc-thiol dextran and the ^{99m}Tc-dextran protein [HSA, MH1 Fab′, MH1 F(ab′)$_2$] complexes were similar and comparable with that of ^{99m}Tc-GHA.

Overall, comparisons of ^{99m}Tc-MH1 Fab′ and ^{99m}Tc-dextran-MH1 Fab′ necropsy data and areas under the curve indicate that a significant improvement in background clearance was obtained using a ^{99m}Tc-dextran derivative to radiolabel MH1 Fab′.

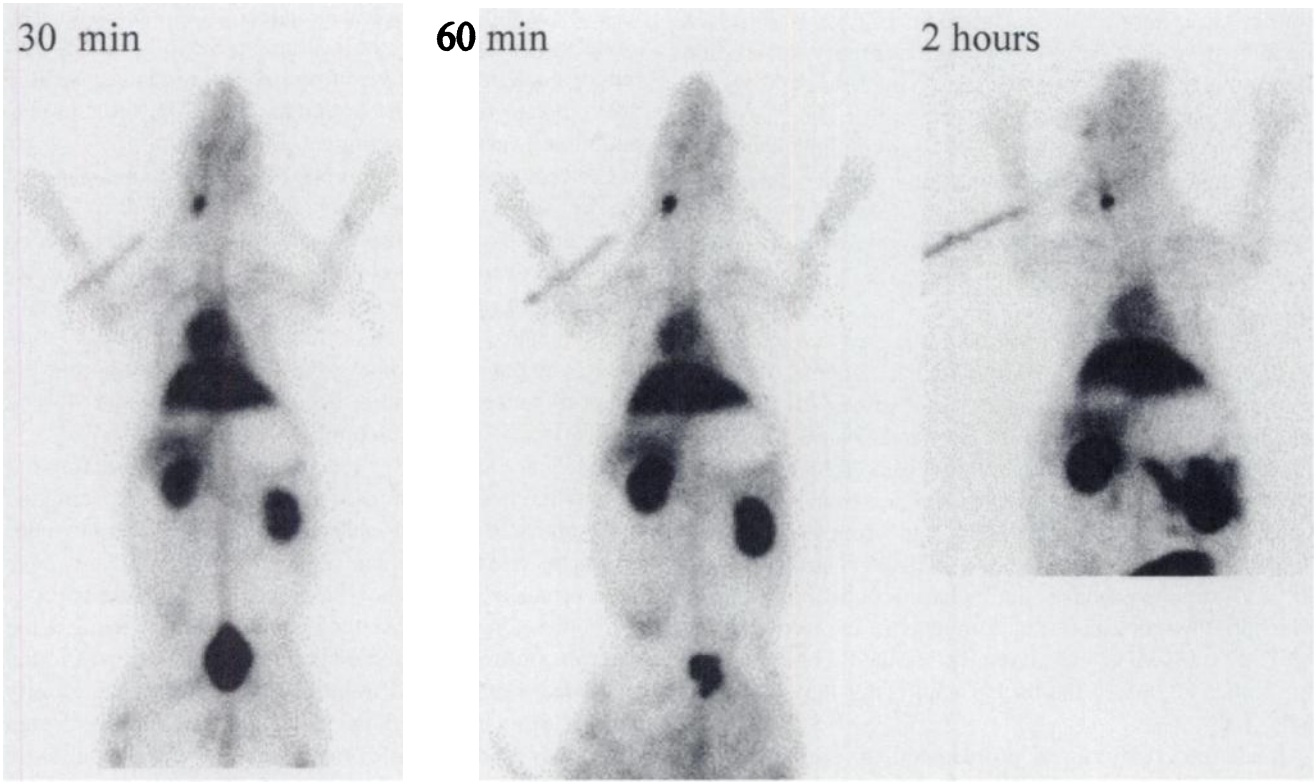

FIGURE 3. Localization of ^{99m}Tc-dextran MH1 Fab′ in jugular clot at 30 and 60 min and 2 h. At 30 min, tracer is evident in liver and kidneys. At 30 min, 33.4% of activity is present in kidney and bladder. Clot uptake is prominent, and tissue background activity is low. By 60 min, heart activity drops significantly and lung background activity is minimal. Rabbit voided between 30 and 60 min. Image obtained at 2 h shows urinary contamination at lower edge of field.

TABLE 1
Comparison of Total and Extravascular Activity in Sprague-Dawley Rat Necropsy Tissues at 1 Hour and Area Under Curve for Image Region Time (0–60 Minutes) Versus ^{99m}Tc Activity

	%ID/g					Extravascular %ID/g				Area under curve, 0–60 min			
^{99m}Tc compound	Blood	Lung	Heart	Muscle	Liver	Lung	Heart	Muscle	Liver	Lung	Heart	Muscle	Liver
GHA (6 studies)	0.110 (0.019)	0.083 (0.016)	0.039 (0.010)	0.029 (0.013)	0.078 (0.013)	0.051 (0.016)	0.027 (0.009)	0.027 (0.012)	0.054 (0.013)	4.1 (0.1)	5.2 (0.4)	3.2 (0.6)	9.2 (0.7)
Dextran-thiol (4 studies)	0.383 (0.049)	0.199 (0.014)	0.109 (0.013)	0.041 (0.009)	0.936 (0.260)	0.088 (0.025)	0.064 (0.007)	0.035 (0.008)	0.855 (0.254)	5.2 (2.0)	15.3 (4.2)	3.3 (0.8)	20.6 (8.2)
Dextran-HSA (9 studies)	0.373 (0.157)	0.171 (0.075)	0.090 (0.039)	0.051 (0.062)	0.446 (0.185)	0.062 (0.047)	0.046 (0.024)	0.045 (0.061)	0.367 (0.158)	4.9 (0.5)	14.8 (1.1)	2.7 (1.1)	18.3 (1.8)
Dextran-MH1 Fab′ (8 studies)	0.531 (0.211)	0.283 (0.082)	0.147 (0.031)	0.042 (0.010)	0.591 (0.174)	0.129 (0.077)	0.085 (0.011)	0.034 (0.010)	0.478 (0.216)	4.4 (0.5)	19.1 (2.5)	2.6 (0.7)	22.8 (1.1)
MH1 Fab′ (11 studies)	0.989* (0.276)	0.715* (0.259)	0.244* (0.045)	0.061 (0.026)	1.165† (0.496)	0.427* (0.198)	0.128* (0.025)	0.046 (0.024)	0.954† (0.494)	6.8 (4.3)	24.9* (3.9)	3.3 (0.9)	40.7* (10.3)
P748 (3 studies)‡	0.79 (0.30)	0.97 (0.34)	0.37 (0.10)	0.05 (0.01)	4.0 (0.64)								

*Value is different ($P < 0.05$) from all dextran compounds and GHA using ANOVA with Newman-Keuls multiple range test.
†Value is different ($P < 0.05$) from dextran-MH1 Fab′ using ANOVA with Newman-Keuls multiple range test.
‡Data are from Lister-James et al. (*18*).
Data are mean and SD (in parentheses) of total number of studies.

DISCUSSION

Thromboembolic disease has an estimated incidence of 5 million cases per year in the United States (*14*). Noninvasive imaging procedures have suboptimal sensitivity and specificity for this life-threatening disease. To improve the diagnosis of pulmonary embolism, new clot-targeting radiopharmaceuticals are needed with faster and more complete thoracic background clearance. Antibodies and peptides have been developed with high binding affinities for thrombus components but, during the first 1–4 h, show persistent thoracic background activity that hinders pulmonary embolism detection.

We have developed a molecular strategy to lower image background activity for intravascular targets. We have studied ^{99m}Tc-dextran because it is restricted to the blood pool and is broken down by the liver and cleared through the kidneys. These properties allow low background activity in the extravascular space and rapid clearance from the intravascular space. ^{99m}Tc-dextran-MH1 Fab′ couples the fibrin specificity of MH1 Fab′ to the clearance characteristics of ^{99m}Tc-dextran to produce a radiopharmaceutical that appears to inherit the properties of its components. In our studies, the ^{99m}Tc-dextran-MH1 Fab′ complex retained its high affinity for clots and cleared the background better than did ^{99m}Tc-MH1 Fab′.

Background activity is problematic, in part because it shrouds the target. In a planar scintigraphic image, clot uptake must be differentiated from background activity in an anteroposterior column of lung and chest wall tissue. Any activity in this column lowers clot contrast, i.e., the target-to-background ratio. Furthermore, nonspecific vascular activity in large or dilated vessels can appear more intense than in vessels containing a clot. Although SPECT studies can reduce background activity from overlying planes, SPECT does little to resolve the problems caused by the complex pulmonary vascular anatomy.

Clot contrast can be improved by either increasing clot uptake or reducing background activity. Clot uptake is determined by tracer affinity for the clot and by local blood flow. Improvements in clot affinity may not proportionally increase clot uptake because tracer delivery can be significantly reduced in a vessel occluded by a thrombus. Alternatively, any reduction in background activity will improve the target-to-background ratio, because local vascular flow is not likely to be a factor that limits background removal.

A primary strategy for reducing blood-pool background activity has been to increase renal clearance by reducing the molecular size of a radiopharmaceutical. For example, Fab′ fragments and recombinant single-chain Fv fragments have been produced to enhance the rate of renal elimination of antibodies. One such construct, comprising only the variable domains of the monoclonal antibody MA-I5C5, was found to bind to immobilized fragment D-dimer with an affinity constant similar to that of the intact antibody but was cleared from the blood 40-fold faster (*15*). Unfortunately, Fv fragments suffer from a high rate of diffusion into extravascular tissues (*16*). For globular antibody fragments and peptides used in thrombus detection, an unfortunate trade-

off is apparent. As molecular weight falls and blood-pool clearance increases, a partially offsetting increase in soft tissue background occurs because of extravascular tracer diffusion. Even for molecules as large as Fab′ fragments, pulmonary extravascular flux is significant. For example, model data indicate that 56% of pulmonary Fab′ fragment molecules distribute to interstitial and cell-associated spaces (*17*). For comparison, in data reported by Lister-James, et al. (*18*) (Table 1), the %ID/g values showed higher residual activity in the lung, heart, and liver for P748 (platelet glycoprotein IIb/IIIa receptor–binding peptide) than for either MH1 Fab′ or thiol dextran-MH1 Fab′. This higher activity may be caused by a high extravascular flux of the agent. At 1 h, for example, P748 activity in the lung was higher than that in the blood (*18*). Thus, blood-pool clearance was not equivalent to image background clearance. Tracers with short blood-residence times that move out of the blood into the soft tissues will still shroud the target in nonspecific image activity.

Fortunately, the intravascular location of thrombi provides a critical advantage that can be exploited to reduce extravascular background activity. Specifically, background noise from extravascular tissues can be avoided if the tracer remains within the blood. Dextran, for example, has been used as a plasma expander because it is a hydrophilic molecule that does not pass the phospholipid bilayer of endothelial cell membranes. On the other hand, the string-like quality of dextran facilitates its passage through the renal glomeruli, especially when the chain length has been reduced by hepatic enzymes (*3,19*). Dextran has a well-established safety, biodistribution, metabolism, and clearance profile (*4–6,19–22*) and has low immunogenicity (*2,4*). Dextran is not concentrated by any body tissue (*6,21*), is broken down by hepatic α-1,6-glucosidase at a rate of 70 mg/kg/d (*4*), and is eliminated from the blood through the kidneys. The biochemistry and mass of a targeting molecule usually determine its biodistribution and the rate of background clearance. For ^{99m}Tc-MH1 Fab′, molecular mass (~55 kD) reduces renal clearance. The properties of dextran can be used to advantage for radiolabeling an intravascular targeting molecule. The dextran portions of nontargeted radiopharmaceutical are broken down and rapidly eliminated. Because the antifibrin antibody in ^{99m}Tc-dextran MH1 Fab′ is not radioactive, it does not contribute to image background activity. Hence, target contrast is significantly improved through reduction of nontargeted background activity.

CONCLUSION

Taken together, the in vivo studies in the rat model suggest that radiolabeling of MH1 Fab′ with ^{99m}Tc-dextran derivatives results in low nonspecific blood and tissue background activity. The data show that ^{99m}Tc-dextran-MH1 Fab′ has lower lung, heart, and liver localization at 1 h than does the directly radiolabeled antibody fragment. The lower background activity of the dextran-labeled complex can potentially enhance clot contrast and improve the detection of thromboemboli.

The technology of ^{99m}Tc-dextran radiolabeling may also improve detection of other clinically important fixed intravascular targets, such as tumor vascular antigens, signals of endothelial inflammation and infection, and atherosclerosis-associated antigens. Because the factors influencing the breakdown and clearance of dextran appear independent of the nature of a small number of attached molecules, labeling with cleavable dextran derivatives may enhance the diagnostic function of a variety of monoclonal antibodies, antibody fragments, peptides, and receptor-related intravascular targeting molecules.

ACKNOWLEDGMENTS

The authors thank Renita Singh, Theresa Daugherty, Sean Osser, and Daniel Bauer for valuable technical support with the in vitro and in vivo experiments.

REFERENCES

1. Sherwood RF, Baird JK, Atkinson T, Wiblin CN, Rutter DA, Ellwood DC. Enhanced plasma persistence of therapeutic enzymes by coupling to soluble dextran. *J Biochem.* 1977;164:461–464.
2. Klotz U, Kroemer H. Clinical pharmacokinetic considerations in the use of plasma expanders. *Clin Pharmacokinet.* 1987;12:123–135.
3. Mehvar R, Robinson MA, Reynolds JM. Molecular weight dependent tissue accumulation of dextrans: in vivo studies in rats. *J Pharm Sci.* 1994;83:1495–1499.
4. Mishler JM. Synthetic plasma volume expanders: their pharmacology, safety and clinical efficacy. *Clin Haematol.* 1984;13:75–92.
5. Nishikawa M, Yamashita F, Takakura Y, Hashida M, Sezaki H. Demonstration of the receptor-mediated hepatic uptake of dextran in mice. *J Pharm Pharmacol.* 1992;44:396–401.
6. Yamaoka T, Kuroda M, Tabata Y, Ikada Y. Body distribution of dextran derivatives with electric charges after intravenous administration. *Int J Pharm.* 1995;113:149–157.
7. Bayley H, Standring DN, Knowles JR. Propane-1,3-dithiol: a selective reagent for the efficient reduction of alkyl and aryl azides to amines. *Tetrahedron Lett.* 1978;39:3633–3634.
8. Dubois M, Gilles KA, Hamilton JK, Rebers PA, Smith F. Colorimetric method for determination of sugar and related substances. *Anal Chem.* 1956;28:530–356.
9. Habeeb AFSA. Determination of free amino groups in proteins by trinitrobenzene sulfonic acid. *Anal Biochem.* 1966;14:328–336.
10. Lei K, Ruszkowski M, Chang F, Qu T, Mardirossian G, Hnatowich DJ. Technetium-99m antibodies labeled with MAG3 and SHNH: an in vitro and animal in vivo comparison. *Nucl Med Biol.* 1996;23:917–922.
11. Rhodes BA, Zamora PO, Newell KD, Valdez EF. Technetium-99m labeling of murine monoclonal antibody fragments. *J Nucl Med.* 1986;27:685–693.
12. Knight LC, Maurer AH, Ammar IA, Shealy DJ, Mattis JA. Evaluation of indium-111-labeled anti-fibrin antibody for imaging vascular thrombi. *J Nucl Med.* 1988;29:494–502.
13. Line BR, Herrmannsdoerfer AJ, Battles AH, Weber PB, Dansereau RN, Blumenstock FA. Premortem biodistribution of radioactivity in the rat: measurement of blood and tissue activity of tracers used in clinical imaging studies. *Lab Anim Sci.* 1994;44:495–502.
14. Moser KM. Venous thromboembolism. *Am Rev Respir Dis.* 1990;141:235–249.
15. Laroche Y, Demaeyer M, Stassen JM, et al. Characterization of a recombinant single-chain molecule comprising the variable domains of a monoclonal antibody specific for human fibrin fragment D-dimer. *J Biol Chem.* 1991;266:16343–16349.
16. Holvoet P, Collen D. Immunoscintigraphy of thrombi [editorial] *J Nucl Med.* 1991;32:2321–2323.
17. Covell DG, Barbet J, Holton OD, Black CD, Parker RJ, Weinstein JN.

Pharmacokinetics of monoclonal immunoglobulin G1, F(ab')2, and Fab' in mice. *Cancer Res.* 1986;46:3969–3978.
18. Lister-James J, Vallabhajosula S, Moyer BR, et al. Pre-clinical evaluation of technetium-99m platelet receptor-binding peptide. *J Nucl Med.* 1997;38:105–111.
19. Mehvar R, Shepard TL. Molecular-weight-dependent pharmacokinetics of fluorescein-labeled dextrans in rats. *J Pharm Sci.* 1992;81:908–912.
20. Stock RJ, Cilento EV, McCuskey RS. A quantitative study of fluorescein isothiocyanate-dextran transport in the microcirculation of the isolated perfused rat liver. *Hepatology.* 1989;9:75–82.
21. Nishida K, Mihara K, Takino T, et al. Hepatic disposition characteristics of electrically charged macromolecules in rat in vivo and in the perfused liver. *Pharm Res.* 1991;8:437–444.
22. Mehvar R, Reynolds JM. Pharmacokinetics of 70-kilodalton fluorescein-dextran in experimental diabetes mellitus. *J Pharmacol Exp Ther.* 1993;264:662–669.